DOI: 10.1002/chem.200800870

New Insight into the Mode of Action of Nickel Superoxide Dismutase by Investigating Metallopeptide Substrate Models

Daniel Tietze,[a] Hergen Breitzke,[a] Diana Imhof,[b] Erika Kothe,[c] James Weston,[d] and Gerd Buntkowsky*[a]

Abstract: For the first time, the existence of a substrate adduct of a nickel superoxide dismutase (NiSOD) model, based on the first nine residues from the N terminus of the active form of *Streptomyces coelicolor* NiSOD, has been proven and the adduct has been isolated. This adduct is based on the cyanide anion (CN^-), as a substrate analogue of the superoxide anion ($O_2^{\bullet-}$), and the nickel metallopeptide H-HCDLPCGVY-NH_2-Ni. Spectroscopic studies, including IR, UV/Vis, and liquid- and solid-state NMR spectroscopy, show a single nickel-bound cyanide anion, which is embedded in the metallopeptide structure. This complex sheds new light on the question of whether the mode of action of the NiSOD enzyme is an inner- or outer-sphere mechanism. Whereas discussion was previously biased in favor of an outer-sphere electron-transfer mechanism due to the fact that binding of cyanide or azide moieties to the nickel active site had never been observed, our results are a clear indication in favor of the inner-sphere electron-transfer mechanism for the disproportionation of the $O_2^{\bullet-}$ ion, whereby the substrate is attached to the Ni atom in the active site of the NiSOD.

Keywords: enzyme catalysis · nickel · substrate binding · superoxide dismutase

Introduction

Reactive oxygen species (ROS), such as superoxide anions ($O_2^{\bullet-}$), are generated in aerobic organisms in which molecular oxygen is reduced by reactive metabolites of the respiratory chain.[1] These ROS can cause severe metabolic malfunctions and damage biological macromolecules like DNA by peroxidation.[2] Superoxide dismutases (SODs; EC 1.15.1.1) destroy the superoxide anion radical by converting it into hydrogen peroxide and oxygen with a rate near the diffusion limit ($k_{cat} > 2 \times 10^9\ M^{-1} s^{-1}$).[3–5] Initially, two independent classes of SODs were identified. They contain either a dinuclear Cu or Zn cofactor or a mononuclear Fe or Mn cofactor.[2] Later, the third class of nickel-containing SODs was discovered in *Streptomyces* by Youn et al.[6–8] NiSOD, as a mononuclear Ni-containing metalloenzyme, cycles between the Ni^{II} and Ni^{III} oxidation states during catalysis.[4,9,10] Two crystallographic and several spectroscopic studies have given an impression of the structure of the whole enzyme and the geometry of its active site.[4,9–11] The X-ray crystallographic analysis of the SODs from *S. seoulensis* (1.68 Å resolution) and *S. coelicolor* (1.30 Å) reveal differences between their structures in the secondary coordination sphere.[9,12] Both show a hexameric quaternary structure, with each monomeric unit containing an isostructural active site with a single covalently bound nickel ion. The coordination geometry of the active site is shown in Scheme 1.[9,10,13] With respect to the mode of action, Maroney and co-workers and Wuerges et al. investigated different NiSOD mutants and demonstrated that the axial His1 imidazole group is vitally important in optimizing the rate of

[a] M. Sc. D. Tietze, Dr. H. Breitzke, Prof. Dr. G. Buntkowsky
Friedrich-Schiller-Universität Jena
Institut für Physikalische Chemie
Helmholtzweg 4, 07743 Jena, (Germany)
Fax: (+49) 3641-948302
E-mail: gerd.buntkowsky@uni-jena.de

[b] Dr. D. Imhof
CMB Zentrum für Molekulare Biomedizin
Institut für Biochemie und Biophysik
Hans-Knöll-Str. 2
07745 Jena (Germany)

[c] Prof. Dr. E. Kothe
Friedrich-Schiller-Universität Jena
Institut für Mikrobiologie
Neugasse 25, 07743 Jena (Germany)

[d] Prof. Dr. J. Weston
Universidad Nacional de La Plata
Facultad de Ciencias Exactas
Centro de Química Inorgánica
47 y 115, C. C. 962–1900 La Plata (Argentina)

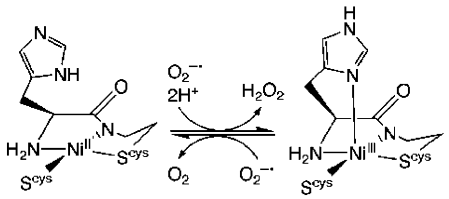

Scheme 1. Coordination geometry and catalytic scheme.[15]

the $O_2^{\bullet-}$ conversion.[3,10] These results were corroborated by hybrid DFT studies by Pelmenschikov and Siegbahn.[14]

As well as inorganic nickel complexes, Shearer and co-workers prepared several metallopeptide NiSOD models that were based on the first 12 or 7 residues, respectively, from the N terminus of the active form of *S. coelicolor* NiSOD. In contrast to all of the inorganic model compounds, these peptide-based NiSOD model compounds exhibited catalytic activity.[15,16] In analogy to the enzyme mutants investigated by Maroney and co-workers and by Wuerges et al., Shearer and co-workers also analyzed several mutants of the heptamer metallopeptide, in which the His1 residue was replaced by Asp or Ala, respectively. For both heptamer metallopeptide mutants, a significantly lower SOD activity was observed in comparison with that of the parent metallopeptide.[10] However, in contrast to the results with the native enzyme, the catalytic activity was not completely diminished by the loss of the His residue as an axial ligand. At the same time, Weston and co-workers examined several SOD-active metallopeptides based on the first six and nine residues, respectively, from the N terminus of the NiSOD from *S. coelicolor*. The 3D NMR solution structure of the peptide exhibits, in contrast with the *cis* Leu4–Pro5 bond in the NiSOD enzyme, a *trans* Leu4–Pro5 bond.[17] Weston and co-workers concluded that this finding could have a strong effect on the comparability of the proposed catalytic mechanisms of the synthetic metallopeptides and the native NiSOD enzyme.

Sequence modification of this hexamer metallopeptide revealed that the imidazole side chain of His1 is, in contrast with the conclusion of Shearer and co-workers, nonessential for the function of the metallopeptide, because the catalytic activity does not disappear completely when the His residue is replaced by Ala. Furthermore, DFT calculations indicate that the carbonyl group in the Pro5–Leu4 peptide bond probably assumes the role of the fifth ligand (Figure 1) and forces substrates to approach the nickel center from the opposite side as compared to the situation with the native enzyme.[17]

To shed light on the opposing opinions regarding the suggested mechanisms and the manner of inhibition with cyanide ions as discussed by Barondeau and co-workers[9] for both the native enzyme and the metallopeptides, we decided to develop and analyze stable substrate models derived from the metallopeptides of Shearer, Weston, and their respective co-workers.[15–17] Our present work is focused on the synthesis and characterization of a stable metallopeptide–cyanide adduct based on nine residues from the N terminus of the active form of *S. coelicolor* NiSOD. For solid-state and liquid NMR spectroscopy and IR experiments, we prepared different cyanide adducts by using unlabeled or labeled (98% ^{13}C or ^{15}N) cyanide. By considering the position of the coordinating cyanide ion (1 and/or 2; see Figure 1), we searched for evidence to support one of the two proposed mechanisms.

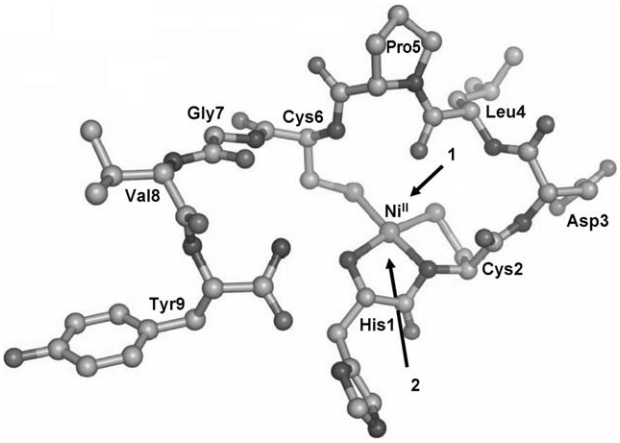

Figure 1. Metallopeptide structure (based on the NMR structure[17]) showing the possible cyanide positions (1 and/or 2) and the possible ligation by the oxygen atom of the Leu4–Pro5 amide bond caused by the *trans* conformation of the peptide.

Results and Discussion

The model peptide (H-HCDLPCGVY-NH_2, mSOD) was prepared in good yield by a standard solid-phase peptide synthesis (SPPS) protocol, according to the 9-fluorenylmethoxycarbonyl (Fmoc) strategy, followed by purification with semipreparative HPLC. Before addition of $NiCl_2$ to the peptide solution, the peptide content (the concentration of the solution) was determined by amino acid analysis and Ellman's reagent.[18] The formation of the metallopeptide by adding $NiCl_2$ (1 equiv) to the peptide seemed to be pH dependent, as described earlier.[15] During titration with 0.1 M NaOH from an initial pH value of around 3 (pH value of the lyophilized peptide) up to a pH value of 7.8, the color of the solution changed from colorless to light pink. The color change occurred between pH 5.5 and 6. Also, mSOD coordinates only a single Ni^{II} ion, as determined by ESI mass spectrometry, which confirms earlier literature findings.[15] The preparation of the cyanide adduct of the metallopeptide was carried out as follows. Upon addition of KCN (1 or 2 equiv, with respect to the peptide content) to the pink-colored metallopeptide solution, the color changed immediately to light yellow, which is a characteristic color for Ni^{II}–cyanide complexes.[19] The major goals of the following investigations were to prove the existence of cyanide ligands directly bound to the nickel, to determine the coordination site of

the cyanide ligand, and to determine the number of coordinating cyanide ions.

After addition of one equivalent of KCN to the metallopeptide, the mass spectra of the obtained complex were recorded. The mass spectrometric experiments with methanolic solutions (negative-ion detection) showed two peaks. The first peak (m/z 1087, 80%) is attributed to the metallopeptide–monocyanide complex [M^-]. The second peak is attributed to the complex [M^-−H+Na] (m/z 1109.0, 100%). Due to the square-planar coordination sphere around the Ni^{II} center in our metallopeptide, there should be enough space for two cyanide ions to form an octahedral coordination geometry, with one cyanide ion above and the second cyanide ion below the coordination plane (Figure 1). In spite of this, we could not find evidence for a bicyanide adduct in the ESI mass spectra (positive- and negative-ion detection) when two equivalents of KCN were added to the nickel(II) nonapeptide solution. To support these findings, we applied UV/Vis, IR, and solid-state NMR spectroscopy.

The electronic absorption spectra are displayed in Figure 2. The spectra for [Ni(mSOD)] recorded in the region of 16000–30000 cm^{-1} are in good agreement with those obtained for other NiSOD metallopeptides.[15,16] The band at 22000 cm^{-1} (454 nm; $\varepsilon = 432\ M^{-1}cm^{-1}$) in the electronic absorption spectra was identified by Shearer and coworkers and by Fiedler et al. as a dd-Ni($3d_{xy}$)/S(π)*→ Ni($3d_{x^2-y^2}$/S/N(σ))* transition, which is characteristic for square-planar $Ni^{II}N_2S_2$ complexes.[11,20,21] The UV region in Figure 2 shows only one broad band centered around 38167 cm^{-1} (262 nm; $\varepsilon = 10787\ M^{-1}cm^{-1}$) and a shoulder at 44843 cm^{-1}. The previously reported shoulder at around 28000 cm^{-1} did not appear in our measurements, which may be because of our use of water/NaOH instead of buffer solutions. Upon addition of KCN to the metallopeptide to generate the cyanide adduct, nearly all of the transitions shift into the UV region. In contrast to the results with the cyanide-free metallopeptide, we observed only one transition in the visible region, at 24390 cm^{-1} (410 nm; $\varepsilon = 177\ M^{-1}cm^{-1}$). The most intense band shifts from 38167 to 39682 cm^{-1} (252 nm; $\varepsilon = 11846\ M^{-1}cm^{-1}$) and shows, in contrast with the broad band of the cyanide-free metallopeptide, a very distinct shoulder at around 35460 cm^{-1} (282 nm). As shown in Figure 2, the addition of two equivalents of KCN to the metallopeptide has no effect on the spectra. To support our interpretation and exclude the formation of $K_2[Ni(CN)_4]$, we recorded the spectra of neat $K_2[Ni(CN)_4]$ as a control experiment. The resulting UV/VIS spectrum is clearly distinct from the spectra obtained for the [Ni(CN)(mSOD)] or [$Ni(CN)_2$(mSOD)] samples. The fact that we could not observe a significant change between the spectra of the cyanide adduct upon addition of one or two equivalents of KCN led us to suggest that only a single cyanide–metallopeptide species exists. The spectra also indicate that CN^- does not remove the nickel atom from the peptide by forming the tetracyano nickelate ion.[9] Further evidence was obtained by employing IR spectroscopy to analyze the bonding character of the cyanide ion by investigating the relative position of the C–N stretching vibration mode (ν_{CN}).[22]

Figure 3 shows the sections of the IR spectra that contain the cyanide band. For KCN, $K_2[Ni(CN)_4]$, and our cyanide adduct [Ni(CN)(mSOD)], we found different values of ν_{CN}. The value of the C–N stretching mode for the supposed cyanide adduct is located somewhere between the corresponding values for free CN^- and for $K_2[Ni(CN)_4]$. The different intensities of the ν_{CN} bands are caused by the different concentrations in the KBr pellets (Figure 3). From the absence of the $K_2[Ni(CN)_4]$ signal in the IR spectra of our cyanide adduct, it is evident that the cyanide-adduct sample does not contain the tetracyano nickelate ion in significant amounts.

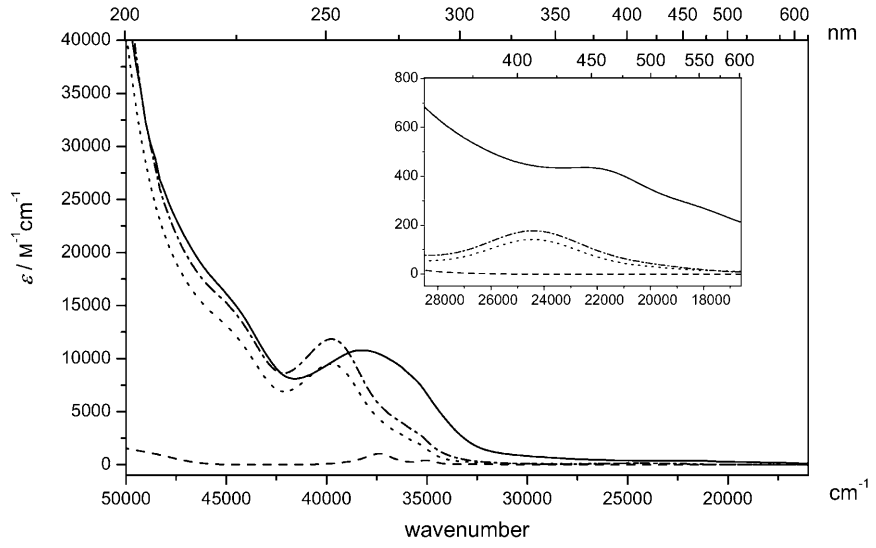

Figure 2. UV/Vis spectra of [Ni(mSOD)] (——), [Ni(CN)(mSOD)] (–•–•), [$Ni(CN)_2$(mSOD)] (-----), and $K_2[Ni(CN)_4]$ (– – –) equivalents of KCN added (water/NaOH, pH 7.8, 20°C). The inset displays an enlargement of the 13000–30000 cm^{-1} region.

In the next step, the IR spectrum of the cyanide adduct formed with two equivalents of KCN was studied. Two KBr pellets were prepared with nearly equal concentrations of [Ni(mSOD)] and with one or two equivalents of KCN added (Figure 4). The absorbance of the C–N stretching vibrational mode was increased by the factor of 1.52 when two equivalents of KCN were added to the sample. This increase is a strong hint that only a single cyanide ion is bonding to the nickel center of our metallopeptide. If a second cyanide ion attached to the nickel center, a second band, caused by the changed coordination geometry (probably square-pyramidal to octahe-

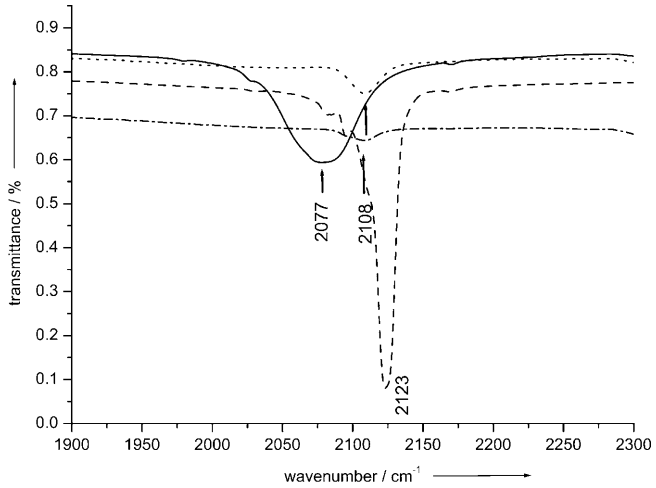

Figure 3. IR spectra of KCN (——), $K_2[Ni(CN)_4]$ (– – –), [Ni(CN)-(mSOD)] (-----), and $[Ni(CN)_2(mSOD)]$ (–•–•) (freeze-dried powder from water/NaOH, pH 7.8, as KBr pellets).

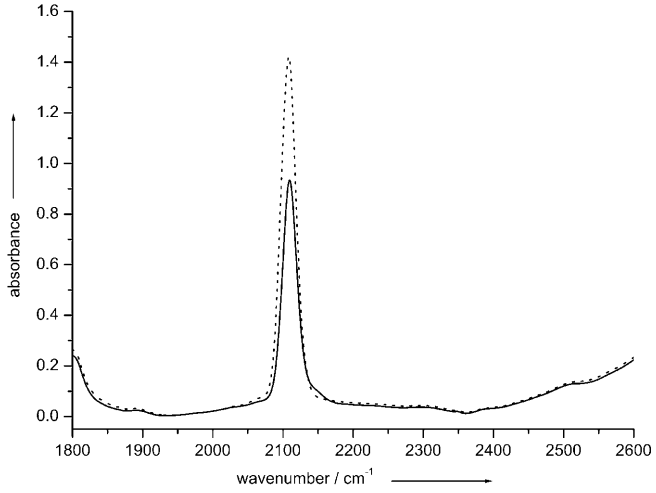

Figure 4. Mass-corrected IR spectra of the metallopeptide–cyanide adduct with one (——) or two (-----) equivalents of KCN added (freeze-dried powder from water/NaOH, pH 7.8, as KBr pellets).

Table 1. ν_{CN} data taken from the IR spectra and reference data from the literature.[23,24]

	ν_{CN} [cm^{-1}]
K^{13}CN	2039
KC^{15}N	2046
KCN	2077 (lit. value: 2080)
$K_2[Ni(^{13}CN)_4]$	2076
$K_2[Ni(C^{15}N)_4]$	2092
$K_2[Ni(CN)_4]$	2123 (lit. value: 2124)
[Ni(^{13}CN)(mSOD)]	2063
[Ni(C^{15}N)(mSOD)]	2077
[Ni(CN)(mSOD)]	2108

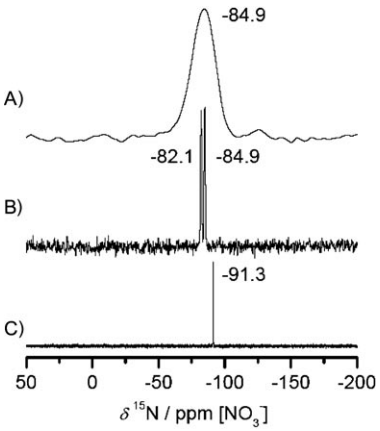

Figure 5. Solid-state ^{15}N-CPMAS NMR spectra of A) [Ni(C^{15}N)(mSOD)] at 25 °C with a spinning rate of 10 kHz; B) $K_2[Ni(C^{15}N)_4]$ at 25 °C with a spinning rate of 10 kHz; C) KC^{15}N at 25 °C with a spinning rate of 5 kHz.

Table 2. Solid-state and solution ^{15}N and ^{13}C NMR data for the chemical shift of the cyanide ion.

		Chemical shift (δ) [ppm]	
		solid state	solution
^{15}N NMR	KC^{15}N	−91.281 (s)	
	$K_2[Ni(C^{15}N)_4]$	−82.167 (s), −84.901 (s)	
	[Ni(C^{15}N)(mSOD)]	−84.917 (s)	
^{13}C NMR	$K_2[Ni(^{13}CN)_4]$	135.968 (t), 140.494 (t)	139.991 (s)
	[Ni(^{13}CN)(mSOD)]	136.126	135.943 (s)

dral), would appear. This behavior leads to the conclusion that cyanide binding to the metallopeptide is incomplete if only one equivalent of KCN is used. Using ^{13}C- or ^{15}N-enriched cyanide, we observed the behavior expected for the ν_{CN} band according to the isotopic effect (Table 1).

Further insight into the structure of the complex was obtained by high-resolution liquid- and solid-state NMR spectroscopy by employing selectively ^{13}C- and ^{15}N-isotope-labeled samples.

The single-pulse solid-state ^{15}N NMR spectra (Figure 5) reveal different chemical shifts for the nitrogen atoms of the cyanide groups of KC^{15}N and $K_2[Ni(C^{15}N)_4]$; these values are collected in Table 2. The ^{15}N signal of $K_2[Ni(C^{15}N)_4]$ is split into two sharp resonances of equal intensity (Figure 5). To test whether remaining water protons are responsible for this effect, the cross-polarization magic-angle-spin (CPMAS) technique was employed.[25] By means of this technique, it is possible to transfer polarization from highly polarized abundant nuclei (usually ^{1}H) to X nuclei with lower polarizations, such as ^{13}C or ^{15}N, when they are brought into contact and, thus, to distinguish between X nuclei with and without protons in their vicinity.[26] Application of the CPMAS technique on $K_2[Ni(^{13}CN)_4]$ did not yield any ^{13}C signals, which confirmed that all water was removed by freeze drying. The ^{15}N-CPMAS experiment on the [Ni(C^{15}N)(mSOD)] complex gave a different result. A broad ^{15}N signal was observed for the cyanide adduct (Figure 5). Compared to the neat KC^{15}N, the line position is low field shifted to the same chemical-shift value as that observed for the signal of the $K_2[Ni(C^{15}N)_4]$ complex (10 kHz spinning speed). The appearance of a ^{1}H–^{15}N cross-polarization signal is clear evidence that the ^{15}N nuclei are now in

the vicinity of hydrogen nuclei. This and the chemical shift that corresponds to that of neat $K_2[Ni(C^{15}N)_4]$ indicates that cyanide ions are incorporated into the metallopeptide and a stable adduct is formed. The nickel-bound cyanide ion now possesses a dipolar interaction to a proton. By lyophilization, all free water molecules are removed from the sample and only strongly bound water molecules may still exist in the peptide. Owing to their strongly bound nature, it is very improbable that these water molecules are able to form a stable hydrogen bond to the cyanide ions and thus act as a source for the cross-polarization effect. Thus, the source of the cross-polarization signal has to be attributed to the peptide. This interpretation is corroborated by the greatly increased line width of the ^{15}N resonance (neat $K_2[Ni(C^{15}N)_4]$: below 1 ppm; $[Ni(C^{15}N)(mSOD)]$ adduct: approximately 20 ppm). This increase is a strong indication that the cyanide ion is involved in hydrogen bonds to an amide group or another hydrogen-donor group of the peptide backbone, which causes a distribution of isotropic chemical shifts.[27,28]

No difference in the ^{15}N-CPMAS spectra of the metallopeptide–cyanide adduct is observed when two equivalents of cyanide are used. This is understandable if one takes the very long T_1 relaxation time (approximately 1 h) of free $C^{15}N$ into account. For this reason, the ^{15}N spectrum of $KC^{15}N$ was measured as a single-shot experiment of a full (30 mg) rotor.

The above results are corroborated by the ^{13}C spectra. While the neat $K_2[Ni(^{13}CN)_4]$ is only visible in the spectra with single-pulse excitation, the $[Ni(^{13}CN)(mSOD)]$ gives a strong, broad cyanide resonance with a maximum intensity at 136 ppm (Figure 6), which is not visible in the spectrum of the neat mSOD peptide.

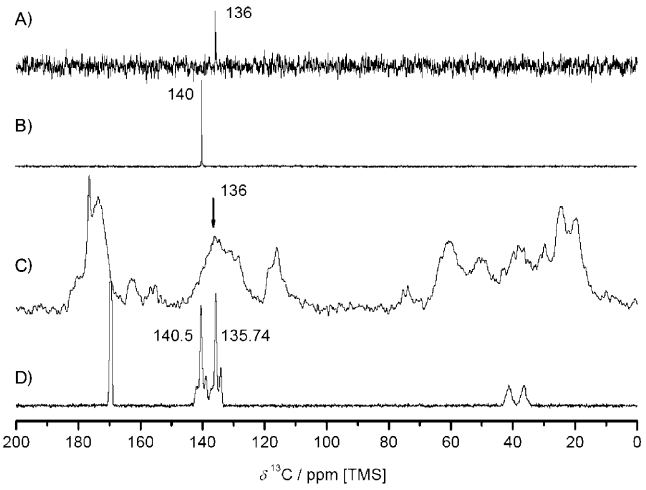

Figure 6. A) ^{13}C NMR spectrum of $[Ni(^{13}CN)(mSOD)]$ in D_2O; B) ^{13}C NMR spectrum of $K_2[Ni(^{13}CN)_4]$ in D_2O; C) solid-state ^{13}C-CPMAS NMR spectrum of $[Ni(^{13}CN)(mSOD)]$ diluted 1:3 with unlabeled [Ni(CN)(mSOD)] at a spinning rate of 10 kHz with the maximum of the ^{13}C signal of $^{13}CN^-$ at 136 ppm; D) solid-state ^{13}C-MAS NMR spectrum of $K_2[Ni(^{13}CN)_4]$ at a spinning rate of 10 kHz. The narrow peak at 170 ppm is caused by formic acid, which is a degradation product of KCN.[29] All spectra were recorded at 25 °C.

The next question one has to answer is whether the splitting of the cyanide resonance in both the solid-state ^{15}N- and solid-state ^{13}C-MAS spectra of $K_2[Ni(C^{15}N)_4]$ and $K_2[Ni(^{13}CN)_4]$ is caused by chemically inequivalent cyanide ions in the $K_2[Ni(C^{15}N)_4]$ and $K_2[Ni(^{13}CN)_4]$, by scalar couplings, or by crystal effects that render the cyanide ions inequivalent in the solid state. This question can be answered by regular liquid-state ^{13}C NMR spectra. The ^{13}C NMR spectra of both $K_2[Ni(^{13}CN)_4]$ and $[Ni(^{13}CN)(mSOD)]$ in solution reveal only a single line; this shows that the observed splitting is a crystal effect. The different number of lines in the liquid- and solid-state ^{13}C NMR spectra of $K_2[Ni(^{13}CN)_4]$ is due to distortion of the $[Ni(CN)_4]^{2-}$ ion in the solid state. Dry $K_2[Ni(CN)_4]$ crystallizes in a monoclinic structure with space group $P21/c$, which results in two distinct C–N bond lengths within the $[Ni(CN)_4]^{2-}$ ion.[30] This effect is also observed in $K_2[Pd(CN)_4]$, which possesses the same crystal structure as $K_2[Ni(CN)_4]$.[24]

The question now is how many cyanide ions bind to the [Ni(mSOD)] peptide. The square-planar local environment of the Ni center implies that, in principle, up to two cyanide ions could bind to the [Ni(mSOD)], one above and one below the local symmetry plane. Since the perfect symmetry is slightly distorted by the peptide environment, these two cyanides are chemically inequivalent and should give two separate signals in high-resolution liquid-state NMR spectra. The NMR spectroscopic results (Figure 6) clearly indicate a single nickel-bound cyanide ion. Thus, one of the two sides is clearly preferred by the cyanide ions. As discussed above, this cyanide ligand is attached through a hydrogen bond to a hydrogen donor of the peptide, that is, most probably, to an amide function.

These results are in contradiction with the crystallographic binding studies performed by Getzoff and co-workers on the native enzyme.[9] They found that neither CN^- nor N_3^- binds to the nickel center of the native enzyme. Neupane and Shearer also treated their metallopeptide with CN^- ions and did not observe cyanide-adduct formation under their chosen conditions (pH 7.4, *N*-ethylmorpholine buffer solution).[16] Furthermore, they described that, if more than four equivalents of NaCN are added to a solution of their metallopeptide, it completely strips the Ni^{II} ion from the peptide.

These contradictory results are understandable by assuming that the formation of the [Ni(CN)(mSOD)] complex is in competition with the formation of $[Ni(CN_4)]^{2-}$. The $[Ni(CN_4)]^{2-}$ complex, with its high equilibrium constant of $7.1 \times 10^{21}\,L^3mol^{-3}$ in aqueous solution,[31] seems to be thermodynamically favored compared to the metallopeptide. Thus, at cyanide concentrations larger than two equivalents relative to the peptide concentration, the nickel ions are extracted from the peptide and form the $[Ni(CN_4)]^{2-}$ complex. On the other hand, our results show that, at stoichiometric concentrations (1 equiv), cyanide ions are indeed able to coordinate at the nickel active site of the metallopeptide in a stable manner. Since the local geometry of the nickel ion is not or, at most, is only weakly affected by the length of the remaining peptide chain, we conclude that the same result

of cyanide binding should be found for the peptides studied by Weston, Shearer, and their respective co-workers, as long as an excess of CN ions is avoided. Moreover, we also draw the conclusion that, under similar conditions, such coordination should also be possible for the native enzyme.

This result has important consequences for the interpretation of the reaction mechanism of NiSOD. Previously, the discussion was biased more to an outer-sphere than an inner-sphere electron-transfer mechanism, due to the fact that binding of cyanide or azide ligands to the nickel active site had never been observed.[9,11,16] With our demonstration of a stable complex of cyanide ions and a peptide-based substrate model complex of NiSOD, the discussion about the NiSOD mechanism now has to be modified in favor of an inner-sphere electron-transfer mechanism.

Finally, the question arises of where exactly the cyanide ligand is coordinating. Calculations by Weston and co-workers predict that one side is less accessible than the other side,[17] which corroborates our result of a strongly preferred binding to one side. To identify this side and the peptide residue that is hydrogen bonded to the cyanide ion, a detailed solid-state NMR study of the binding is currently being performed in our laboratory.

Conclusion

For the first time, the existence of a stable substrate adduct of a metallopeptide-based NiSOD model substance has been proven. Under stoichiometric conditions, [Ni(mSOD)] easily forms a stable cyanide adduct. The use of one or two equivalents of KCN does not have a significant effect on the spectroscopic data. MS and NMR data demonstrate that only a single cyanide ion is attached to the nickel center. NMR experiments reveal that this cyanide ion forms at least one hydrogen bond to the peptide backbone. This shows that the cyanide ion is not only fixed within the peptide structure of the metallopeptide by electrostatic forces.

Experimental Section

Infrared spectroscopy was performed on a Bruker IFS 66 spectrometer.-UV/Vis measurements were recorded on a Varian Cary 5000 UV/Vis/NIR spectrophotometer by using quartz cuvettes with 1 cm pathlength. All solutions were prepared from doubly distilled water with a pH value of 7.8. Solid-state NMR measurements were carried out on a Bruker Avance II+ spectrometer at 400 MHz proton frequency by utilizing a Bruker 3.2 mm HFXY probe under MAS conditions and with various spinning rates. CPMAS sequences, as well as a 90° single pulse, have been employed. Liquid-state NMR spectroscopy was performed on a Bruker Avance II+ 400 spectrometer. The ^{13}C spectra are referenced with respect to tetramethylsilane (TMS) and ^{15}N spectra are referenced with respect to NO_3^-. For more details, see the figure legends of the corresponding spectra. Mass spectra were recorded by using an SSQ 710 Finigan MAT instrument. The purity of the peptide was assessed by analytical HPLC by using a Shimadzu LC-10AT system equipped with a reversed-phase Vydac 218TP column (25×4.6 mm, 5 μm) and a gradient of 10→50% eluent B over 40 min (A: 0.1% trifluoroacetic acid (TFA) in water; B: 0.1% TFA in acetonitrile) at a flow rate of 1 mL min^{-1} (t_R = 19.1 min). For the purification of the crude peptide, a semipreparative Shimadzu LC-8A HPLC system equipped with a Eurospher 100 C18 column (Knauer, 250×32 mm, 5 μm) was used. Elution was performed with a gradient of 15→65% eluent B over 120 min (B: 0.1% TFA in 9:1 acetonitrile/water) at a flow rate of 10 mL min^{-1} (t_R = 35 min). All chromatograms were recorded at 254 nm by using a Shimadzu UV/Vis detector. Unless otherwise stated, all amino acid derivates, coupling reagents, and resins were purchased from Orpegen Pharma or Novabiochem and used without further purification.

Synthesis of H-HCDLPCGVY-NH$_2$ (mSOD): The nonapeptide was synthesized by using standard manual Fmoc SPPS on Rink amide MBHA (4-(2′,4′-dimethoxyphenyl-Fmoc-aminomethyl)-phenoxyacetamido-norleucyl-4-methylbenzhydrylamine) resin with a loading capacity of 0.58 mmol g^{-1} and with 1-hydroxy-1*H*-benzotriazole (HOBt)/*O*-(benzotriazol-1-yl)-*N*,*N*,*N*′,*N*′-tetramethyluroniumhexylfluorophosphate (HBTU; 4 equiv each relative to loading capacity) or diisopropylcarbodiimide (DIC; 4 equiv relative to loading capacity) coupling reagents. The base diisopropylethylamine (DIEA) was used in twofold excess compared to the amino acids and coupling reagents. Cleavage from the resin was achieved with 95% TFA, 2.5% triisopropylsilane, and 2.5% water. The peptide was precipitated in cold diethyl ether, washed several times, and freeze dried prior to purification by semipreparative HPLC and storage at −80 °C. HPLC: t_R = 19.1 min (analytical); 35 min (preparative); ESI MS (+ve ion): *m*/*z* (%): 1005 (80) [M^+−H], 1027 (100) [M^++Na], 1048 (20) [M^++K].

Synthesis of [Ni(mSOD)]: Complexation with Ni^{II} and CN^- ions was performed under inert conditions. Millipore water was degassed and saturated with argon. For the solid-state NMR spectroscopy experiments, it was necessary to avoid the use of buffer solutions.

mSOD (9.6 mg; peptide content 67% as determined by amino acid analysis and Ellman's reagent) was dissolved in water (5 mL) to give a 1.28 mM peptide solution. $NiCl_2$ (0.345 mL, 0.0185 M, 1 equiv) was added in accordance with the peptide content calculated by the Ellman's test.[18] During the process of adjusting the pH value to 7.8 with a computer-controlled titrator (0.1 M NaOH; Methrom Titrino DMS 716), a slightly pink solution was formed. This solution was subsequently freeze dried. ESI MS (+ve ion): *m*/*z* (%): 1063.2 (100) [M^++H], 1085.2 (20) [M^++Na]; UV/Vis (water, pH 7.8): λ_{max} (ε) = 546 (sh), 454 (432), 262 (10787 mol^{-1} cm^{-1}), 223 nm (sh).

Synthesis of [Ni{CN(^{13}CN,C^{15}N)}(mSOD)]: Before the pH value of the metallopeptide solution was adjusted to 7.8, a freshly prepared 0.02 M KCN solution in water (0.317 mL, 1 equiv, or 0.634 mL, 2 equiv; Acros) was added. Upon both cyanide additions, a slightly yellow solution was formed, which was then freeze dried. The preparation of the labeled compounds was performed under the same conditions by using K^{13}CN or KC^{15}N (98% enriched, Chemotrade Chemiehandelsgesellschaft mbH, Leipzig).

[Ni(CN)(mSOD)]: ESI MS (− ion): *m*/*z* (%): 1109.0 (100) [M^-−H+Na], 1087 (80) [M^-−H]; IR (KBr): ν = 2108 cm^{-1} (C≡N); UV/Vis (water, pH 7.8): λ_{max} (ε) = 410 (176), 282 (sh), 252 (11846 mol^{-1} cm^{-1}), 223 nm (sh).

[Ni(C^{15}N)(mSOD)]: ESI MS (−ve ion): *m*/*z* (%): 1110.0 (100) [M^-−H+Na], 1088 (70) [M^-−H]; IR (KBr): ν = 2077 cm^{-1} (C≡N); ^{15}N NMR (400 MHz, solid state, 25 °C, NO_3^-): δ = −84.257 ppm (s, Ni−C^{15}N).

[Ni(^{13}CN)(mSOD)]: ESI MS (−ve ion): *m*/*z* (%): 1110.0 (100) [M^-−H+Na], 1088 (76) [M^-−H]; IR (KBr): ν = 2063 cm^{-1}; ^{13}C NMR (400 MHz, solid state, 25 °C, TMS): δ = 136.126 ppm (Ni−^{13}CN); ^{13}C NMR (400 MHz, D_2O, 25 °C, TMS): δ = 135.943 ppm (s, Ni−^{13}CN).

Synthesis of K$_2$[Ni{CN(^{13}CN,C^{15}N)}$_4$]: $NiCl_2 \cdot 6H_2O$ (98 mg, 0.41 mmol) was dissolved in water (1 mL), and KCN (54 mg, 0.82 mmol; Acros; or, if appropriate, K^{13}CN or KC^{15}N, 98% enriched, Chemotrade Chemiehandelsgesellschaft mbH, Leipzig) was added. The nickel biscyano complex was formed as a green precipitate and washed twice with water (1 mL). To form the tetracyano nickel(II) complex, further KCN (or K^{13}CN or KC^{15}N; 80 mg, 1.2 mmol, 3 equiv) dissolved in water (2 mL) was added

to the green biscyano nickel(II) complex. An orange-yellow solution was formed and was subsequently freeze dried.

$K_2[Ni(CN)_4]$: IR (KBr): $\nu = 2123\ cm^{-1}$ (C≡N); UV/Vis (water, pH 7.8): λ_{max} (ε) = 333 (sh), 310 (65), 285 (409), 268 nm (1048 $mol^{-1} cm^{-1}$).

$K_2[Ni(C^{15}N)]_4$: ^{15}N NMR (400 MHz, solid state, 25 °C, NO_3^-): $\delta = -82.167$ (s, Ni–$C^{15}N$), −84.901 ppm (s, Ni–$C^{15}N$); IR (KBr): $\nu = 2092\ cm^{-1}$ (C≡N).

$K_2[Ni(^{13}CN)]_4$: (400 MHz, solid state, 25 °C, TMS): $\delta = 140.494$ (t, Ni–^{13}CN), 135.968 ppm (t, Ni–^{13}CN); ^{13}C NMR (400 MHz, D_2O, 25 °C, TMS): $\delta = 139.991$ ppm (s, Ni–^{13}CN); IR (KBr): $\nu = 2076\ cm^{-1}$ (C≡N).

Acknowledgements

The Deutsche Forschungsgemeinschaft is acknowledged for their financial support. We thank the research group of Dr. Diana Imhof for support concerning peptide synthesis and peptide analytics and Dr. Antje Kriltz for the IR measurements.

[1] J. S. Valentine, D. L. Wertz, T. J. Lyons, L. L. Liou, J. J. Goto, E. B. Gralla, *Curr. Opin. Chem. Biol.* **1998**, *2*, 253–262.
[2] J. M. Mates, J. M. Segura, C. Perez-Gomez, R. Rosado, L. Olalla, M. Blanca, F. M. Sanchez-Jimenez, *Blood Cells Mol. Dis.* **1999**, *25*, 103–109.
[3] P. A. Bryngelson, S. E. Arobo, J. L. Pinkham, D. E. Cabelli, M. J. Maroney, *J. Am. Chem. Soc.* **2004**, *126*, 460–461.
[4] S. B. Choudhury, J. W. Lee, G. Davidson, Y. I. Yim, K. Bose, M. L. Sharma, S. O. Kang, D. E. Cabelli, M. J. Maroney, *Biochemistry* **1999**, *38*, 3744–3752.
[5] M. Cox, D. Nelson, A. Lehninger in *Lehninger Biochemie*, Springer, Heidelberg, **2001**.
[6] H. D. Youn, E. J. Kim, J. H. Roe, Y. C. Hah, S. O. Kang, *Biochem. J.* **1996**, *318*, 889–896.
[7] T. Eitinger, *J. Bacteriol.* **2004**, *186*, 7821–7825.
[8] A. Schmidt, A. Schmidt, G. Haferburg, E. Kothe, *J. Basic Microbiol.* **2007**, *47*, 56–62.
[9] D. P. Barondeau, C. J. Kassmann, C. K. Bruns, J. A. Tainer, E. D. Getzoff, *Biochemistry* **2004**, *43*, 8038–8047.
[10] J. Wuerges, J. W. Lee, Y. I. Yim, H. S. Yim, S. O. Kang, K. D. Carugo, *Proc. Natl. Acad. Sci. USA* **2004**, *101*, 8569–8574.
[11] A. T. Fiedler, P. A. Bryngelson, M. J. Maroney, T. C. Brunold, *J. Am. Chem. Soc.* **2005**, *127*, 5449–5462.
[12] T. A. Jackson, T. C. Brunold, *Acc. Chem. Res.* **2004**, *37*, 461–470.
[13] J. Wuerges, J. W. Lee, S. O. Kang, K. D. Carugo, *Acta Crystallogr. Sect. D* **2002**, *58*, 1220–1223.
[14] V. Pelmenschikov, P. E. M. Siegbahn, *J. Am. Chem. Soc.* **2006**, *128*, 7466–7475.
[15] J. Shearer, L. M. Long, *Inorg. Chem.* **2006**, *45*, 2358–2360.
[16] K. P. Neupane, K. Gearty, A. Francis, J. Shearer, *J. Am. Chem. Soc.* **2007**, *129*, 14605–14618.
[17] M. Schmidt, S. Zahn, M. Carella, O. Ohlenschläger, M. Görlach, J. Weston, *ChemBioChem* **2008**, *9*, 2135–2146.
[18] G. L. Ellman, *Arch. Biochem. Biophys.* **1958**, *74*, 443–450.
[19] "Die Nickelgruppe": N. Wiberg, E. Wiberg, A. F. Hollemann, in *Lehrbuch der Anorganischen Chemie*, Walter deGruyter, Berlin, **1995**, pp. 1578–1585.
[20] K. P. Neupane, J. Shearer, *Inorg. Chem.* **2006**, *45*, 10552–10566.
[21] J. Shearer, N. F. Zhao, *Inorg. Chem.* **2006**, *45*, 9637–9639.
[22] P. Gans, J. B. Gill, L. H. Johnson, *J. Am. Chem. Soc. Dalton Trans.* **1993**, 345–349.
[23] A. Terzis, K. N. Raymond, T. G. Spiro, *Inorg. Chem.* **1970**, *9*, 2415–2420.
[24] C. Muhle, J. Nuss, R. E. Dinnebier, M. Jansen, *Z. Anorg. Allg. Chem.* **2004**, *630*, 1462–1468.
[25] J. Schaefer, E. O. Stejskal, *J. Am. Chem. Soc.* **1976**, *98*, 1031–1032.
[26] C. P. Slichter, *Principles of Magnetic Resonance*, Springer, Heidelberg, **1990**.
[27] T. Emmler, S. Gieschler, H. H. Limbach, G. Buntkowsky, *J. Mol. Struct.* **2004**, *700*, 29–38.
[28] P. Lorente, I. G. Shenderovich, N. S. Golubev, G. S. Denisov, G. Buntkowsky, H. H. Limbach, *Magn. Reson. Chem.* **2001**, *39*, S18–S29.
[29] G. Jander, E. Blasuis, J. Straehle, *Einführung in das anorganisch-chemische Praktikum*, Hirzel, Stuttgart, **1995**.
[30] N. G. Vannerberg, *Acta Chem. Scand.* **1964**, *18*, 2385–2391.
[31] "Komplex- und Koordinationschemie": E. Riedel in *Moderne Anorganische Chemie*, Walter deGruyter, Berlin, **1999**, pp. 155–325.

Received: May 7, 2008
Published online: November 17, 2008

